Ultrahigh energy density in short-range tilted NBT-based lead-free multilayer ceramic capacitors by nanodomain percolation

JI, Hongfen, WANG, Dawei, BAO, Weichao, LU, Zhilun, WANG, Ge, YANG, Huijing, MOSTAED, Ali, LI, Linhao, FETEIRA, Antonio <http://orcid.org/0000-0001-8151-7009>, SUN, Shikuan, XU, Fangfang, LI, Dejun, MA, Chao-Jie, LIU, Shu-Yu and REANEY, Ian

Electronic Supplementary Information for

Ultrahigh energy density in short-range tilted lead-free multilayer ceramic capacitors by nanodomain percolation

Hongfen Ji[a,b#], Dawei Wang[a*], Weichao Bao[c#], Zhilun Lu[a,d#], Ge Wang[a#], Huijing Yang[a,e], Ali Mostaed[a,f], Linhao Li[a], Antonio Feteira[g], Shikuan Sun[a], Fangfang Xu[c], Dejun Li[h], Chao-Jie Ma[i], Shi-Yu Liu[h*], Ian M. Reaney[a*]

[a]Department of Materials Science and Engineering, University of Sheffield, Sheffield, S1 3JD, UK

[b]Laboratory of Thin Film Techniques and Optical Test, Xi'an Technological University, Xi'an 710032, China

[c]State Key Laboratory of High Performance Ceramics and Superfine Microstructure, Shanghai Institute of Ceramics, Shanghai, 200050, China

[d]The Henry Royce Institute, Sir Robert Hadfield Building, Sheffield, S1 3JD, UK

[e]Department of Physics, Tangshan Normal University, Tangshan 063000, China

[f]Department of Materials, University of Oxford, Oxford OX1 3PH, UK

[g]Materials and Engineering Research Institute, Sheffield Hallam University, Sheffield, S1 1WB, UK

[h]College of Physics and Materials Science, Tianjin Normal University, Tianjin 300387, China

[i]School of Materials Science and Engineering, Beijing Institute of Technology, Beijing 100081, China.

*Corresponding authors. E-mail addresses:

dawei.wang@sheffield.ac.uk, buaasyliu@gmail.com, i.m.reaney@sheffield.ac.uk

[#]Author contributions:

H. Ji, D. Wang, W. Bao, Z. Lu, and G. Wang contributed equally to this work.

Table S1. Tolerance factor (t) and average ionic polarizability (α) for NBT-SBT-xBMN.

Composition	tolerance factor (t)	average ionic polarizability (α, $Å^3$)
0	0.9756	9.0440
0.02	0.9748	9.0727
0.04	0.9739	9.1013
0.06	0.9730	9.1300
0.08	0.9722	9.1587
0.10	0.9713	9.1873

Figure S1. (a) XRD patterns of NBT-SBT-xBMN ceramics ($0 \leq x \leq 0.1$) and enlarged region from 32° to 33° 2θ.

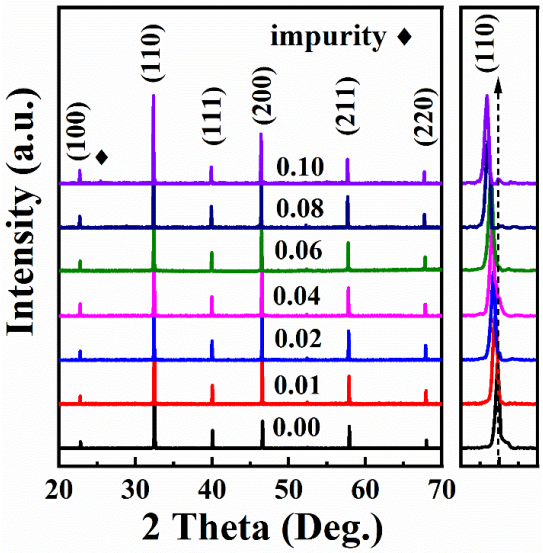

Figure S2. Z”-M” spectroscopic plots for NBT-BT-xBMN ceramics

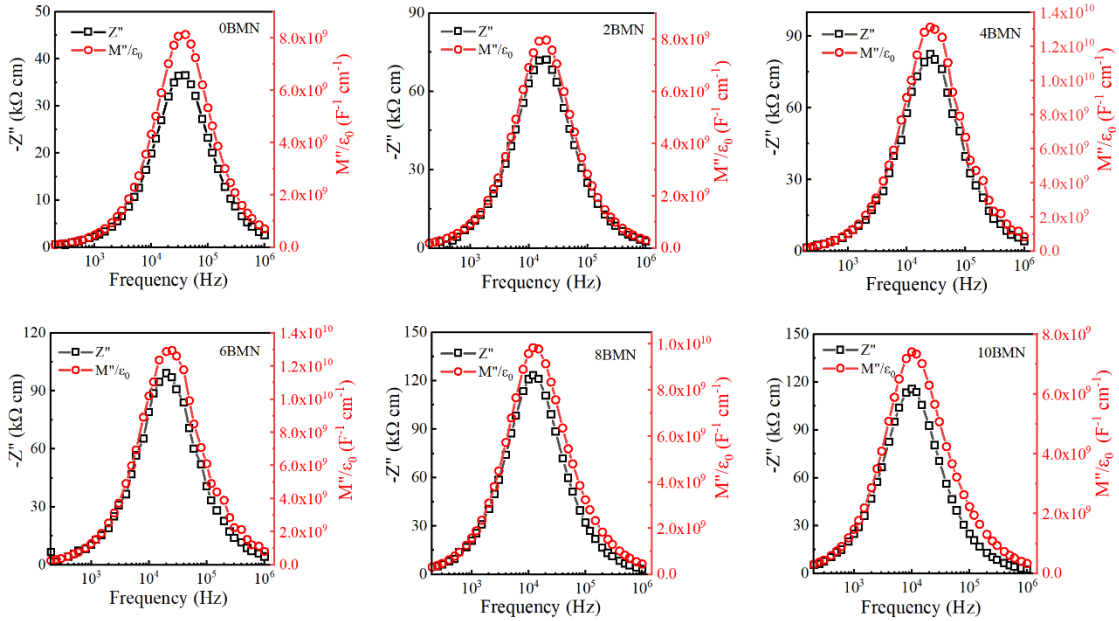

Figure S3. The comparison of P_m, P_r and ΔP studied in this work with other reported energy storage ceramics

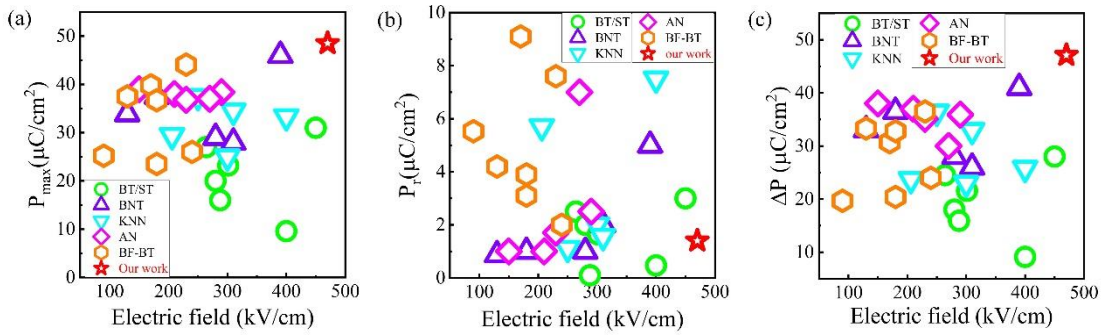

Figure S4. SEM of NBT-SBT-*x*BMN ceramics

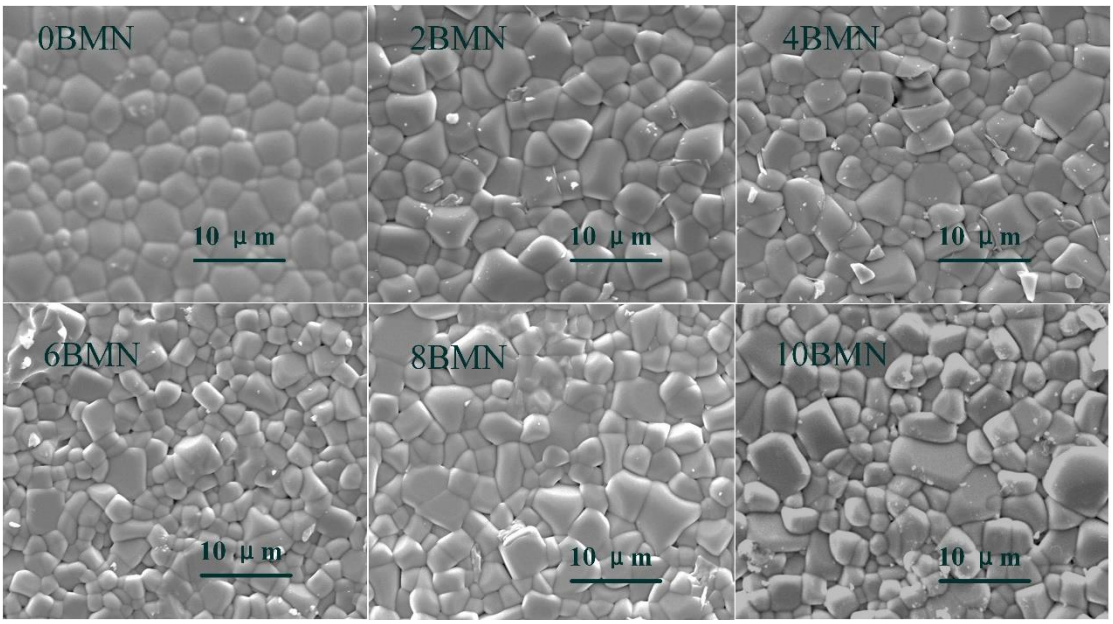

Figure S5. Room-temperature Raman data for NBT-SBT-*x*BMN ceramics

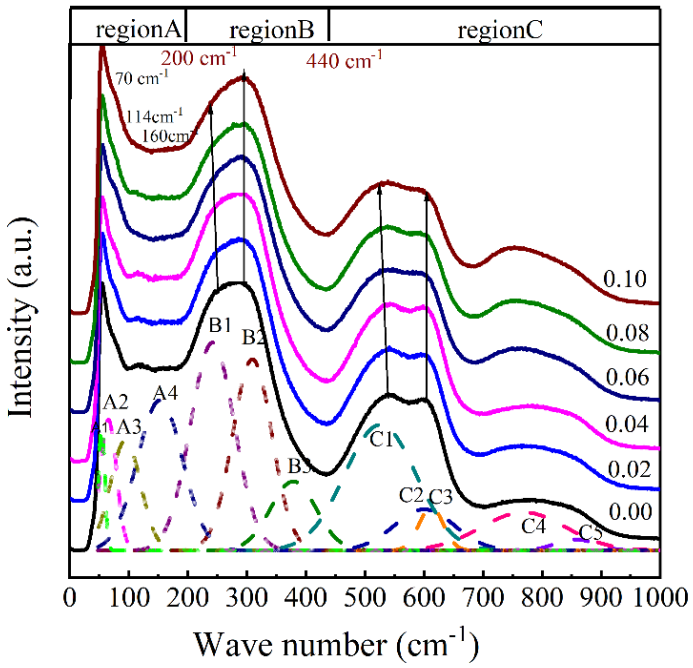

Figure S6. Temperature-dependent dielectric permittivity and loss curves for NBT-0.3SBT-*x*BMN ceramics with different frequencies

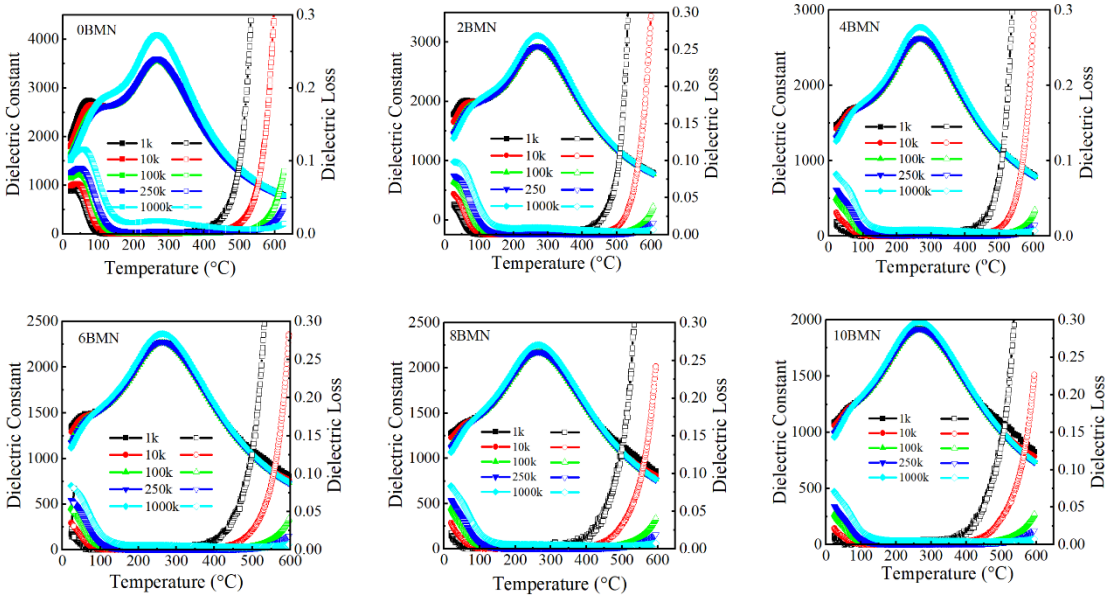

Figure S7. Temperature-dependent dielectric permittivity and loss curves for NBT-BT-*x*BMN ceramics

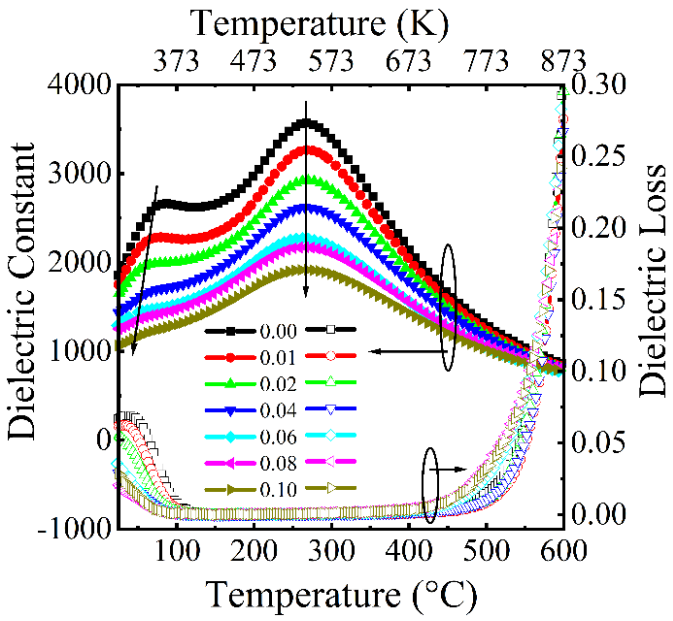

Figure S8. <110> zone axis diffraction patterns of NBT-SBT-0.08BMN, showing ½{hkl} superstructure reflections attributed to antiphase rotations of the O octahedra.

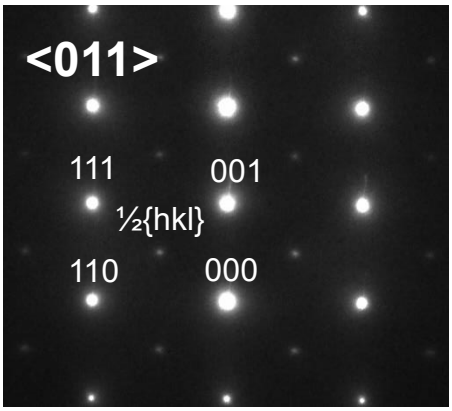

Figure S9. The ε_r/P-E loops for NBT-BT-*x*BMN ceramics

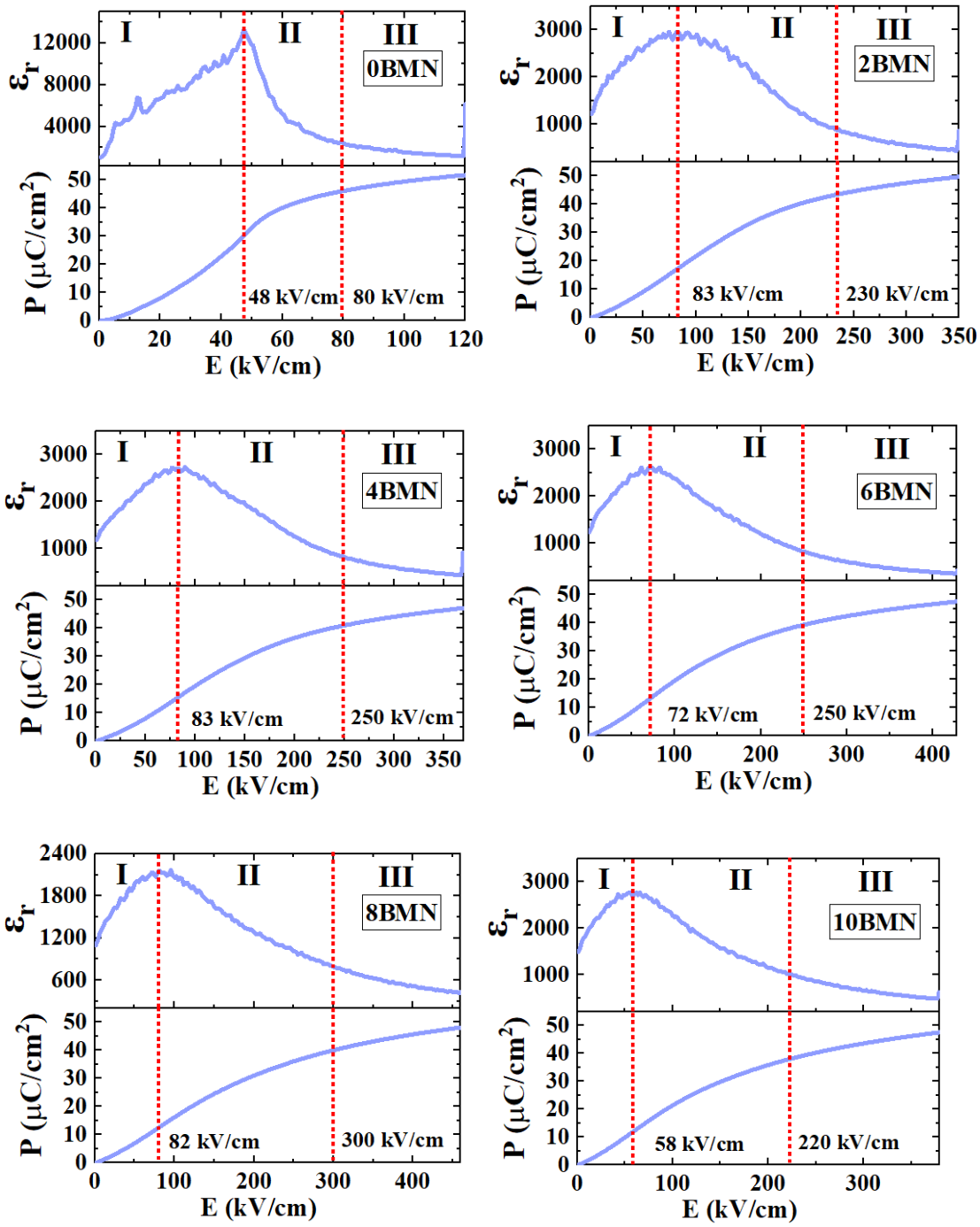

Figure S10. Cross-sectional (a) SEM image, (b) EDX element line element and mapping of (c) Pt and (d) Bi for NBT-SBT-0.08BMN MLCCs.

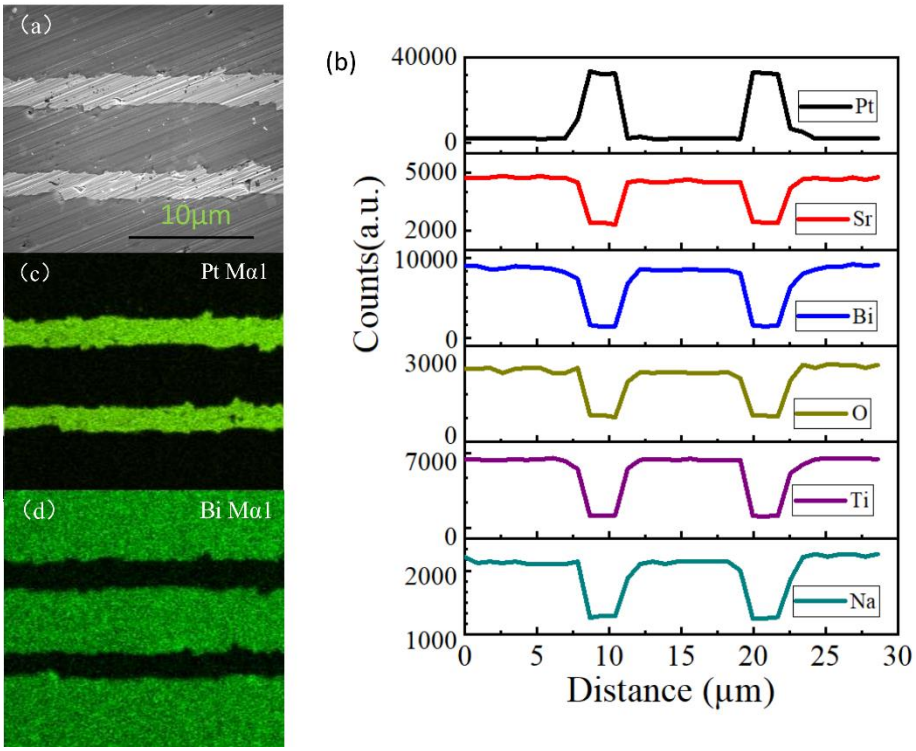

Figure S11. Bright field STEM image and corresponding chemical EDX mapping obtained from an interface between a ceramic grain and a Pt grain (electrode).

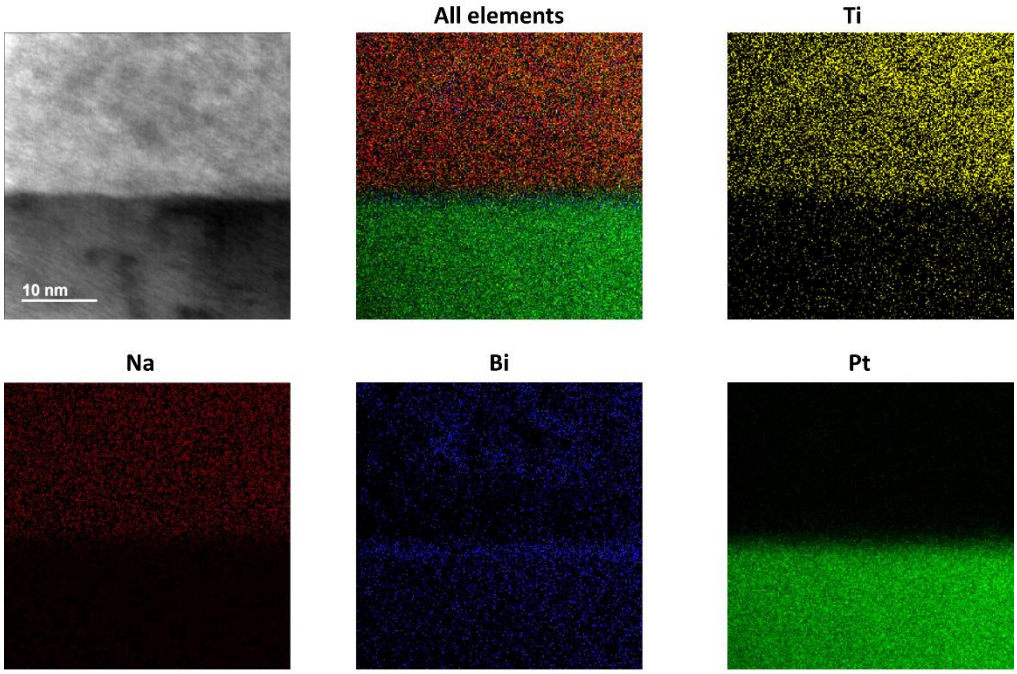

Figure S12. (a) Unipolar P-E loops for NBT-SBT-0.08BMN MLCCs at room temperature; (b) Temperature dependent unipolar P-E loops; (c) Frequency-dependent unipolar P-E loops; (d) AC cycling unipolar P-E loops.

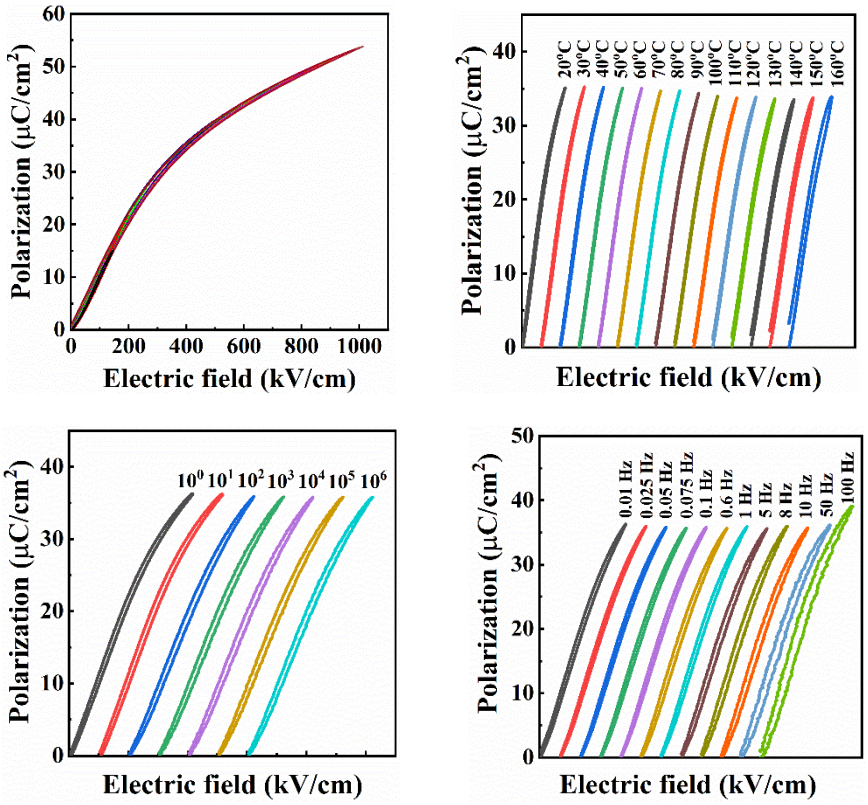

Figure S13. Unipolar strain versus E-field (S-E) loops for NBT-SBT, S_{max} ~ 0.17%, hysteresis ~ 12%, and NBT-SBT-8BMN, S_{max} ~ 0.065%, hysteresis ~ 2.9%